Increasing the Fisher Information Content in the Matter Power Spectrum through Moving-Mesh Reconstruction

Qiaoyin Pan,[1,*] Ue-Li Pen,[2,3,4,5,†] Derek Inman,[2,6] and Hao-Ran Yu[2,7]

[1] *School of Physics, Nankai University, 94 Weijin Rd, Nankai, Tianjin, 300071, China*
[2] *Canadian Institute for Theoretical Astrophysics, University of Toronto, 60 St. George Street, Toronto, Ontario M5S 3H8, Canada*
[3] *Dunlap Institute for Astronomy and Astrophysics, University of Toronto, Toronto, ON M5S 3H4, Canada*
[4] *Canadian Institute for Advanced Research, Program in Cosmology and Gravitation*
[5] *Perimeter Institute for Theoretical Physics, Waterloo, ON, N2L 2Y5, Canada*
[6] *Department of Physics, University of Toronto, 60 St. George, Toronto, ON M5S 1A7, Canada*
[7] *Kavli Institute for Astronomy and Astrophysics, Peking University, Beijing 100871, China*

(Dated: November 25, 2016)

Reconstruction techniques are commonly used in cosmology to reduce complicated non-linear behaviour to a more tractable linearized system. We study the *Moving-Mesh* algorithm which is expected to perform better than many alternatives as it is based in Lagrangian space. To quantify the algorithm's ability to reconstruct linear modes, we study the Fisher information present in 136 N-body simulations before and after reconstruction. We find that the non-linear scale is pushed to $k \simeq 0.3$ h/Mpc after reconstruction as modes between $0.2 \lesssim k/(h/Mpc) \lesssim 0.6$ become less strongly correlated. We furthermore find that the translinear plateau of the cumulative Fisher information is increased by a factor of ~ 40 after reconstruction, from $I \simeq 2.5 \times 10^{-5}/(\mathrm{Mpc}^3/h^3)$ to $I \simeq 10^{-3}/(\mathrm{Mpc}^3/h^3)$ at $k \simeq 1$ h/Mpc. We expect this technique to be beneficial to problems such as baryonic acoustic oscillations and cosmic neutrinos that rely on an accurate disentangling of non-linear evolution from underlying linear effects.

PACS numbers:

I. INTRODUCTION

The power spectrum is widely used in modern cosmology to measure the matter fluctuations. In the early universe, initial Gaussian density fields can be completely described by the power spectrum, or the two-point statistics. However, gravitational instability and nonlinear large scale structure (LSS) formation make the matter distribution highly non-Gaussian, and the galaxy distribution also follows this non-Gaussian distribution. In these cases one needs to compute higher statistics which are computationally more expensive and more difficult to interpret into initial cosmological parameters. Fisher information is usually used to quantify the amount of independent information that is contained in the power spectrum estimation.

Rimes and Hamilton [1] first studied the Fisher information contained in the matter power spectrum given by N-body simulations, and find that there is a plateau on trans-linear scales ($k \simeq 0.2 - 0.8$ h/Mpc), which shows that on these scales, there is a strong coupling of Fourier modes. Thus the power spectrum on smaller scales, gives little additional independent information.

There are many approaches to recover the lost information in the power spectrum of the matter density field, by transforming the final density field into a more Gaussian, early stage density field. For example, Gaussianization transforms are commonly used [2, 3] to make the logarithmic distribution more Gaussian. Nonlinear Wiener filters are used in wavelet space to Gaussianize the fields and can also improve the Fisher information [4–6]. It is shown in [6] that, although these methods or their combinations may have different abilities to recover the Fisher information, by means of reducing the mode coupling and variances in the auto power spectrum of Gaussianized density fields, they do not necessarily improve the cross correlation between the initial density field and the final density field, and thus result in a smearing out of the baryonic acoustic oscillations (BAO) peak in the two-point correlation function. If one is concerned about mapping the initial conditions to final conditions (e.g. measurement of BAO) these methods are unable to extract valid information from initial conditions, at least in the cross power spectrum between initial and final conditions.

Reconstruction techniques (including the one described in [6]) are able to increase the Fisher information while also improving the cross correlation with the initial conditions and sharpening the BAO peak. It is based on the coupling of linear density field $\delta_L(\boldsymbol{q}, t_0)$ to the displacement field $\boldsymbol{\Psi}(\boldsymbol{q})$ (first derived by [7]), which is estimated by a smoothed final density field. [8] shows a new method in the estimation of displacement field in 1-dimensional (1D), according to which the 1D linear density field is reconstructed in Lagrangian space and successfully improves the BAO measurement. In 3D cases, it is nontrivial to estimate the displacement field, but [9] show that the displacement field given by N-body simulations can be used to recover δ_L.

In this paper we generalize the displacement field estimation method from 1D [8] to 3D, reconstruct δ_L and

*Electronic address: panda@mail.nankai.edu.cn
†Electronic address: pen@cita.utoronto.ca

study the Fisher information recovery in δ_L. Here, the displacement field estimation is done by a *Moving-mesh* (MM) algorithm, which is based on the *Adaptive Particle-mesh* (APM) simulation algorithm [10, 11].

This paper is organized as follows. In Section II, we present the main steps of the N-body simulation code that was used to simulate the dark matter density fields. In Section III, we briefly describe the reconstruction algorithm. In Section IV, we calculate and compare the power spectra, correlation matrix and Fisher information given by simulation and reconstruction. The conclusion and discussion are presented in Section V

II. N-BODY SIMULATION OF DARK MATTER DENSITY FIELDS

We use the CUBEP^{3}M [12] to run 136 simulations with a box size of 300 h^{-1}Mpc, afine resolution of 1024^3 cells and 512^3 totally particles. The initial conditions are conputed using the transfer function given by CAMB [13] and then propogating the power linearly back to $z = 100$ with a growth pactor. The Zel'dovich approximation is used to calculate the displacement and velocity fields, which are assigned to the particles. The cosmological parameters used are $\Omega_M = 0.32$, $\Omega_\Lambda = 0.679$, $h = 0.67$, $\sigma_8 = 0.83$, and $n_s = 0.96$. Different seeds are used to produce the initial conditions for different simulations so that they are independent to each other.

III. RECONSTRUCTION ALGORITHM

The basic idea of the MM algorithm is to build a PM scheme on a curvilinear coordinate system, in which the number of particles per grid cell is set approximately constant. Consider a numerical grid of curvilinear coordinates $\boldsymbol{\xi} = (\xi_1, \xi_2, \xi_3)$. In order to determine the physical position of each grid point, one needs to specify the Euclidean coordinate $\boldsymbol{x}(\boldsymbol{\xi}, t)$ as a function of grid position. In the Euclidean coordinate, the flat metric is the Kronecker delta function δ_{ij}, while the curvilinear metric is given by

$$g_{\mu\nu} = \frac{\partial x^i}{\partial \xi^\mu}\frac{\partial x^j}{\partial \xi^\nu}\delta_{ij}. \tag{1}$$

We use the convention that Latin indices denote Cartesian coordinate, while Greek indices denote the curvilinear grid coordinate. In principle, there are many different methods to connect the Cartesian coordinate and curvilinear coordinate of each grid cell. In the APM method, the connection is described by an irrotational deformation,

$$x^i = \xi^\mu \delta^i_\mu + \Delta x^i, \tag{2}$$

where

$$\Delta x^i = \frac{\partial \phi}{\partial \xi^\nu}\delta^i_\nu. \tag{3}$$

This choice of the deformation can minimize mesh distortion and twisting. ϕ is called the deformation potential, and Δx^i the lattice displacement. The deformation potential can be given in terms of the continuity equation in curvilinear coordinates,

$$\frac{\partial(\sqrt{g}\rho)}{\partial t} + \partial_\mu\left[\rho\sqrt{g}e^\mu_i\left(v^i - \Delta\dot{x}^i\right)\right] = 0 \tag{4}$$

where $\sqrt{g} \equiv \det\left|e^i_\mu\right|$ is the volume element and thus $\sqrt{g}\rho$ represents the particle mass in the volume element under the curvilinear coordinate system. The triad is given by $e^i_\mu = \partial x^i/\partial\xi^\alpha$. $\Delta\dot{x}^i = \delta^{i\nu}\partial_\nu\dot{\phi}$ is chosen such that the first term in Eq.4 is zero, resulting in a constant mass per volume element. The velocity field divergence is replaced by the deviation density field $\Delta\rho = \bar{\rho} - \rho\sqrt{g}$, which ideally should be zero. Then the deformation potential is described via the elliptic equation,

$$\partial_\mu(\rho\sqrt{g}e^\mu_i\delta^{i\nu}\partial_\nu\Delta\phi) = \Delta\rho \tag{5}$$

The Eq.5 can be solved using multigrid algorithm described in Ref. [10, 11]. The displacement is then given by the gradiant of the deformation potential as in Eq.3. We run the MM reconstruction code on 136 non-linear density fields from simulation in a resolution of ng= 128 per dimension. The multigrid algorithm is iterated for 1000 times and it rms decreases from roughly 4.5 to roughly 0.2. A 2-D projection of one layer of the deformed grids and the original density field is given in Fig.1. As expected, there is no grid crossing after reconstruction.

IV. POWER SPECTRA AND INFORMATION CONTENT

The power spectrum is the Fourier transform of the correlation function and measures the amount of clustering in the matter distribution as a function of wavenumber k,

$$\langle\delta(\boldsymbol{k})\,\delta(\boldsymbol{k'})\rangle = (2\pi)^3 P(\boldsymbol{k})\,\hat{\delta}(\boldsymbol{k}-\boldsymbol{k'}), \tag{6}$$

where $\delta(\boldsymbol{k})$ is the density fluctuation in wave space, while $\hat{\delta}$ is the delta funciton. Of equal interest is Δ^2_k, the power spectrum in its dimensionless form, defined as

$$\Delta^2(k) \equiv \frac{k^3 P(k)}{2\pi^2} \tag{7}$$

The power spectra of the mass distributions are calculated using the "Nearest Grid Point" (NGP) mass assignment scheme. In Fig.2(a) we plot the mean cross correlation function, $r = P_{\delta\delta_L}/\sqrt{P_\delta P_{\delta_L}}$ of the non-linear and the linear power spectrum, and the reconstructed and linear power spectrum respectively. The wave number where the cross correlation drops to a half increases from $k \simeq 0.2$ h/Mpc to $k \simeq 0.6$ h/Mpc. To qualify the improvement of cross correlation in the power spectrum, we compute the damping factors $\mathcal{D}(k) = r^4$ fitting the Gaussian BAO damping models $\mathcal{D}(k) = \exp(-k^2\Sigma^2/2)$.

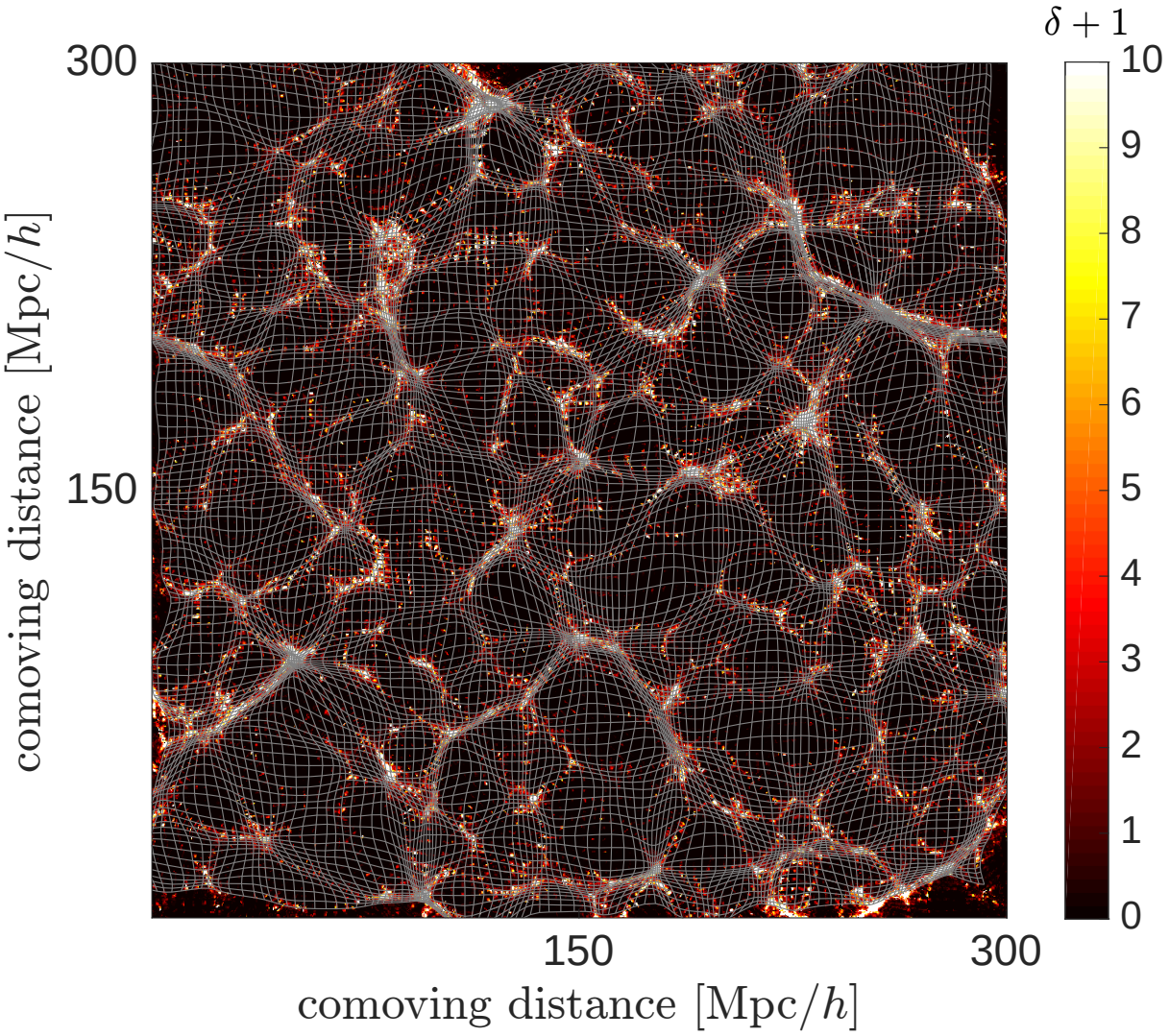

FIG. 1: The 2-D projection of the deformed grid of a sample N-body simulations is shown as curved white lines. The $\delta + 1$ field on the deformed grid is shown underneath.

In Fig.2(a) we plot $\mathcal{D}_{\delta}^{1/4}$ ($\Sigma = 11.3$ Mpc/h) and $\mathcal{D}_{\delta_R}^{1/4}$ ($\Sigma = 3.9$ Mpc/h) over $r_{\delta\delta_L}$ and $r_{\delta_R\delta_L}$. We also plot the $r_{\delta\delta_L}$ and $r_{\delta_R\delta_L}$. We also plot $\mathcal{D}(k)^{1/4}$ that match cross correlation function after E-mode displacement reconstruction (ng = 512, box size = 400 Mpc/h, Σ = 1.3 Mpc/h), which is the result in [9] and MM reconstruction in a higer resolution (ng = 512, box size = 600 Mpc/h, $\Sigma = 2.6$ Mpc/h), which is the result in [14]. We find that with higher resolution, which is more precise, the reconstruction gives a cross correlation damping at smaller scale. And it's expected that the E-mode displacement reconstruction gives a reconstructed power spectrum more correlated with the initial one, since it decomposes completely the irrotational and curl components of the real displacement field in N-body simulation, while the difference between the reconstructed displacement through MM reconstruction and the real displacement still has an irrotational component. In Fig.2(b) we plot the linear power spectrum which is the transfer function, and mean power spectrum (with error bars) of 136 non-linear density fields and reconstruced density fields simply given by $\delta_R(k) = \boldsymbol{k} \cdot \boldsymbol{k}\phi(k)$. The reconstructed power spectrum drops at non-linear scale ($k \gtrsim 0.3\ h$/Mpc) since the reconstructed density fields are totally irrotational. The result is similar to that of E-mode displacement reconstruction described in [9], in which the reconstructed power spectrum drops, but in a different scale and at a different speed.

Mathamatically, the Fisher information [15] I in the log of amplitude A of the initial matter power spectrum is defined as

$$I_A \equiv -\left\langle \frac{\partial^2 \ln \mathcal{L}}{\partial A^2} \right\rangle, \tag{8}$$

in which $\mathcal{L}$ denotes the likelihood. For Gaussian fluctuations, the likelihood depends on parameters only through the power spectrum $P(k)$, and the information I in A de-

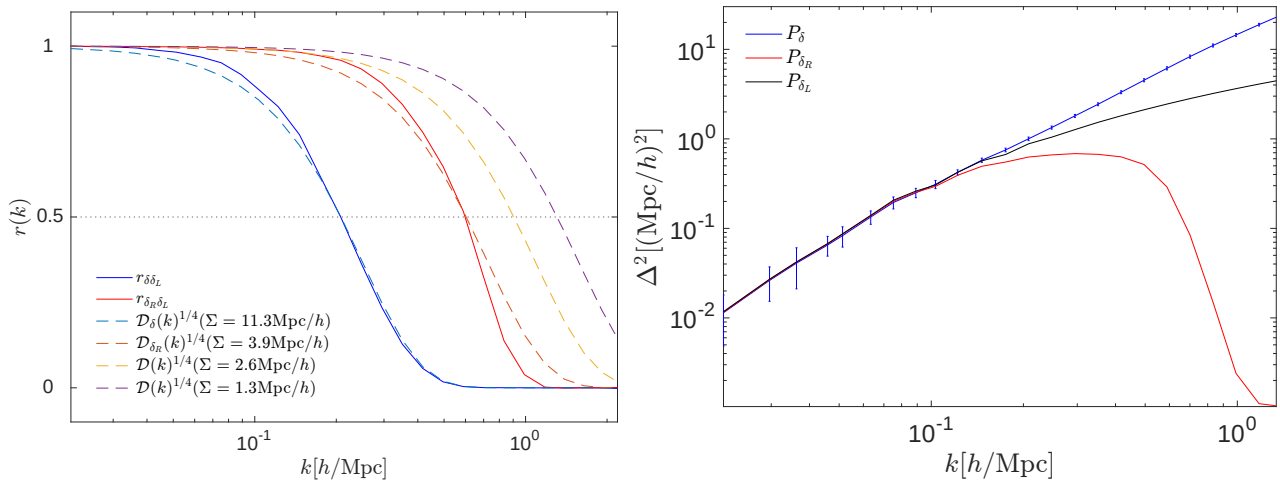

FIG. 2: (a) The cross correlation function (solid lines) $r_{\delta\delta_L}$ (blue) and $r_{\delta_R\delta_L}$ (red), and BAO damping models (dash lines). (b) The dimensionless power spectrum computed via linear theory (black), the mean value of 136 N-body simulations with 1σ error bars (blue), and reconstruction of the simulations (red).

fined by Eq.8 can be written as [1]

$$I_A = -\left\langle \sum_{k,k'} \frac{\partial \ln P(k)}{\partial \ln A} \frac{\partial^2 \ln \mathcal{L}}{\partial \ln P(k) \partial \ln P(k')} \frac{\partial \ln P(k')}{\partial \ln A} \right\rangle, \tag{9}$$

in which the angle bracket denotes the average over all the power spectra.

The definition Eq.9 can be written in a simpler form in two aspects, one of which is the first and the third partial dericative terms. For any density field δ, we can conveniently decompose it into linear and non-linear components

$$\delta(k) = b(k)\delta_L(k) + n(k), \tag{10}$$

in which δ_L denotes the linear density field. $b(k)$ is the bias and $n(k)$ is defined such that the correlation $\langle \delta_L(k) n(k) \rangle$ is zero. If we correlate δ and δ_L,

$$\langle \delta(k)\delta_L(k) \rangle = b(k) \langle \delta_L(k)\delta_L(k) \rangle, \tag{11}$$

we can solve for b as

$$b(k) = \frac{P_{\delta\delta_L}(k)}{P_{\delta_L}(k)}. \tag{12}$$

Non-linear evolution drives $b(k)$ to drop from unity, and generates the non-linear term $n(k)$. Correlating δ and itself,

$$\langle \delta(k)\delta(k) \rangle = b^2(k) \langle \delta_L(k)\delta_L(k) \rangle + \langle n(k)n(k) \rangle, \tag{13}$$

we find

$$P_\delta(k) = \mathcal{D}(k) P_{\delta_L}(k) + P_n(k), \tag{14}$$

where $\mathcal{D}(k) \equiv b^2(k)$ is the non-linear damping factor, and P_n is the mode-coupling term.

With the help of Eq.12 and Eq.14, we can replace the partial derivatives $\partial \ln p(k)/\partial \ln A$ in Eq.9 with

$$\frac{A}{P(k)} \frac{\partial P(k)}{\partial A} = \frac{P^2_{\delta\delta_L}(k)}{P_\delta(k) P_{\delta_L}(k)} \tag{15}$$

which is just the square of the cross correlation function $r^2(k)$, of δ and δ_L.

The second partial derivative terms in Eq.9, the Hessian of the vector $\ln P(k)$, has the expectation value of the Fisher matrix with respect to the log powers. For linear density fields, the Fisher matrix is approximately equal to the inverse of the covariance matrix of power spectrum estimates, which should be diagonal, with diagonal elements equal to the number of modes in each wavenumber bin (when considering $\boldsymbol{k}$ and $-\boldsymbol{k}$ as the same mode). Thus we can write down a simpler matrix product form of cumulative Fisher information,

$$I_A\,(< k_n) = r^2(k)^{\mathrm{T}} \left[\mathrm{C}^{-1}_{\mathrm{norm}}(k, k') \right] r^2(k'), \tag{16}$$

where $\mathrm{C}_{\mathrm{norm}}$ is the normalized covariance matrix with size per dimension up to k_n, defined as

$$\mathrm{C}_{\mathrm{norm}}\,(k, k') = \frac{\mathrm{Cov}(k, k')}{\langle P(k) \rangle \langle P(k') \rangle}, \tag{17}$$

and r is the mean cross correlation of a given density field with linear one as a function of k up to k_n. It's reliable to define Eq.16 for non-linear density fields as well, since the Fisher matrix is approximately the same as that of linear density fields on linear scales. The covariance matrix is defined as

$$\mathrm{Cov}\,(k, k') \equiv \frac{\sum_{i,j=1}^{N} \left[P_i\,(k) - \langle P\,(k) \rangle \right] \left[P_j\,(k') - \langle P\,(k') \rangle \right]}{N - 1}, \tag{18}$$

where angle brackets mean the expected values, and N is the total number of simulations. The cross-correlation

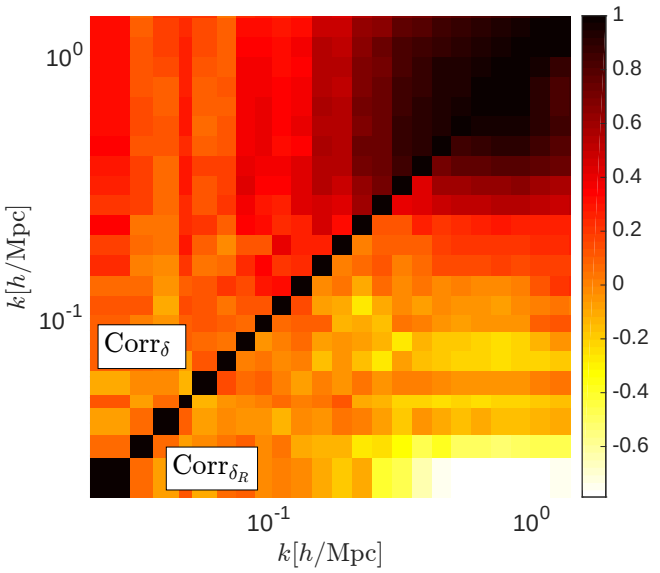

FIG. 3: Correlation coefficient matrix as found from 136 non-linear power spectra (the upper-left elements) and the reconstructed power spectra (the lower-right off-diagonal elements). Both the matrix are symmetric and have unity diagonal elements.

coefficient matrix, or for short the correlation matrix, is the normalized version of the covariance matrix,

$$\mathrm{Corr}\,(k,k') = \frac{\mathrm{Cov}\,(k,k')}{\sqrt{\mathrm{Cov}\,(k,k)\,\mathrm{Cov}\,(k',k')}}, \qquad (19)$$

which represents the correlation between different k modes. The corelation matrices for non-linear and reconstructed power spectra are shown in Fig.3. For the non-linear power spectra, the correlation matrix in the linear regime, $k \lesssim 0.2\ h/\mathrm{Mpc}$, is almost diagonal. The off-diagonal elements are produced by strong mode coupling in non-linear scale, and the super-survey tidal effect which is small on linear scales but dominates in the weakly non-linear regime [16]. The correlation matrix for the non-linear power spectra has few negative elements, ($\mathrm{Corr} \gtrsim -0.1$), which are produced by the unbiased error and thus will vanish with more simulations [17]. For the reconstructed correlation matrix, however, the linear regime expand up to $k \simeq 0.6\ h/\mathrm{Mpc}$, but the number and magnitude of negative off-diagonal elements increases ($\mathrm{Corr} \gtrsim -0.8$).

Cumulative Fisher information is proportional to the volume. We plot the cumulative Fisher information per Mpc^3/h^3 of the non-linear, linear and reconstructed power specta in Fig.4(a). The Fisher information of the non-linear power spectra drops from the linear one at $k \simeq 0.05\ h/\mathrm{Mpc}$, and has a flat plateau in the translinear regime, $k \simeq 0.3\ h/\mathrm{Mpc}$, with a saturated value of $I \simeq 2.5 \times 10^{-5}/(\mathrm{Mpc}^3/h^3)$. It indicates that there's nearly no independent information in the translinear regime of the power spectrum. But the information curve of the reconstructed power spectra keeps incresing roughly the same as the linear information until $k \simeq 0.3\ h/\mathrm{Mpc}$, and reaches it's plateau at $k \simeq 0.8\ h/\mathrm{Mpc}$ with the value of $I \simeq 10^{-3}/(\mathrm{Mpc}^3/h^3)$, up by a factor of 40. It indicates that the MM reconstructed method can strongly recover the lost information within this scale. We compare the Fisher information given by the MM reconstruction method with the logarithmic density mapping method [3] as an example to illustrate their strength. We find that the MM reconstruction gives more than 10 times more information than logarithmic mapping. In some papers, the cross correlation r^2 terms are set to be unity in Eq.16, which apparantly increases the non-linear information. We also plot those in Fig.4(b) for better comparison. But we find that in this case, the MM reconstructed and logarithmic mapping information in the scale $k \simeq 0.2$ - $0.5\ h/\mathrm{Mpc}$ is higher than the linear one, which is not expected.

V. CONCLUSION AND DISCUSSION

The new reconstruction method successfully recovers the lost linear information on the mildly non-linear scale, increasing the saturated information from $I \simeq 2.5 \times 10^{-5}/(\mathrm{Mpc}^3/h^3)$ to at least $I \simeq 10^{-3}/(\mathrm{Mpc}^3/h^3)$, and pushing the non-linear scale to higher k. The result is better than previous methods (e.g. [3–5, 18, 19]), and we believe that the reconstructed Fisher information will further increase to a greater magnitude in smaller scale since the cross correlation of the reconstructed power spectrum with linear one increases in a higher resolution analysis [14]. The result in dark matter density fields gives a strong motivation to adapt the MM reconstruction to halo fields, neutrino fields, etc, so that we have access to the physics in smaller scales. Reconstruction technique are concerned to improve cosmology measurements of BAO scale (e.g. [20, 21]). The successful application of the MM reconstruction on BAO reconstruction in 1-D [8] and 3-D [14] cosmology provides an intuitive view of the algorithm to push forward BAO research.

The MM reconstruction effectively decomposes the irrotational part and the curl part of the displacement field of particles. However, the reconstructed displacement might be greatly different from real displacement in N-body simulation, since it is sensitive to the late stage shell-crossing and non-linear process so that the original position of some spectific particles are replaced by each other. It's meaningful to compare the irrotational displacement field through the MM reocnstruction and that from E-mode displacement reconstruction [9] which decomposes completely the irrotational and curl components of the real displacement in N-body simulation. Since the MM reconstruction only needs the density field input and gives a large recovering of lost information, it's expected to have a good effect on reconstructing the matter density field from observation.

Acknowledgments

We thank Homg-Ming Zhu,Yu Yu and Xin Wang for friendly and helpful discussions. Computations were per-

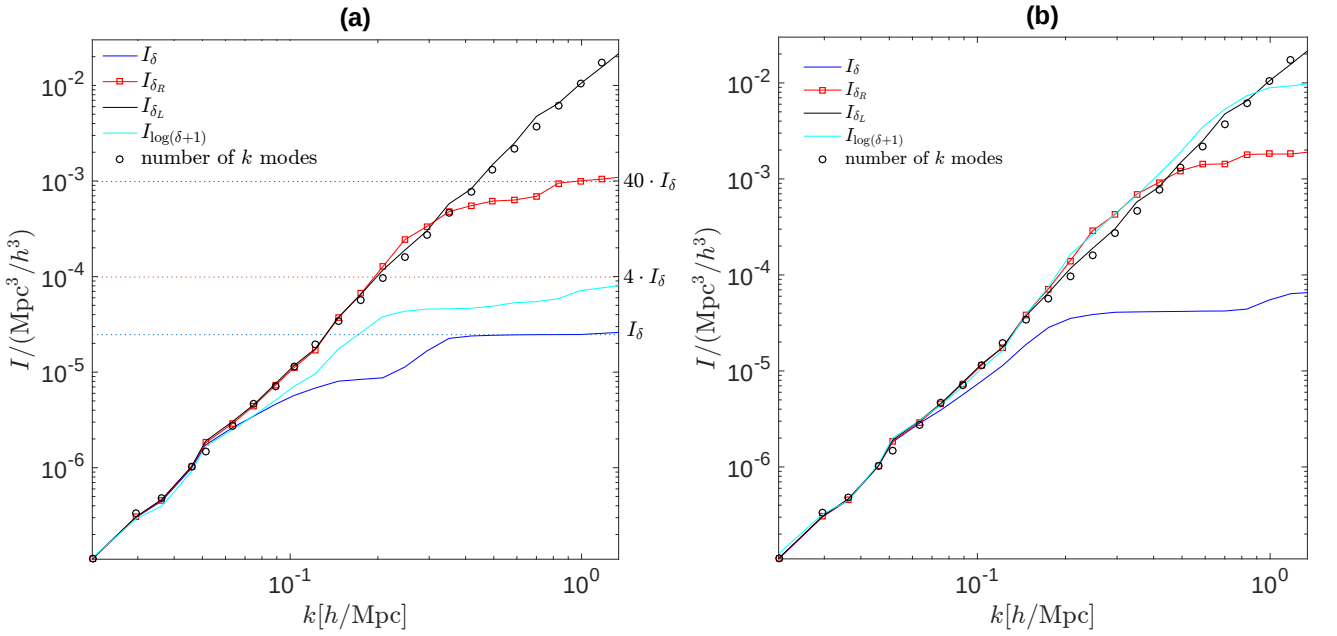

FIG. 4: (a) Cumulative Fisher information per Mpc^3/h^3 in the power spectra as a function of wavenumber. The blue line correspond to the non-linear density field; the red line with squares corresponds to the the reconstructed deformation potential; the dark line corresponds to the linear density field; the circles correspond to number of k modes up to that wave bin. Dotted lines correspond to saturated value of non-linear Fisher information, 4 times and 40 times of it. (b) Cumulative Fisher information per Mpc^3/h^3 given by setting the cross correlation to be unity.

formed on the General Purpose Cluster supercomputer at the SciNet HPC Consortium. SciNet is funded by: the Canadian Foundation for Innovation under the auspices of Compute Canada; the Government of Ontario; Ontario Research Fund - Research Excellence; and the University of Toronto.

[1] C. D. Rimes and A. J. S. Hamilton, in *American Astronomical Society Meeting Abstracts #207* (2006), vol. 207 of *American Astronomical Society Meeting Abstracts*, p. 206.01.
[2] D. H. Weinberg, MNRAS **254**, 315 (1992).
[3] M. C. Neyrinck, I. Szapudi, and A. S. Szalay, ApJ **698**, L90 (2009), 0903.4693.
[4] T.-J. Zhang, H.-R. Yu, J. Harnois-Déraps, I. MacDonald, and U.-L. Pen, ApJ **728**, 35 (2011), 1008.3506.
[5] H.-R. Yu, J. Harnois-Déraps, T.-J. Zhang, and U.-L. Pen, MNRAS **421**, 832 (2012), 1012.0444.
[6] J. Harnois-Déraps, H.-R. Yu, T.-J. Zhang, and U.-L. Pen, MNRAS **436**, 759 (2013), 1205.4989.
[7] Y. B. Zel'dovich, A&A **5**, 84 (1970).
[8] H.-M. Zhu, U.-L. Pen, and X. Chen, ArXiv e-prints (2016), 1609.07041.
[9] H.-R. Yu, U.-L. Pen, and H.-M. Zhu, ArXiv e-prints (2016), 1610.07112.
[10] U.-L. Pen, ApJS **100**, 269 (1995).
[11] U.-L. Pen, ApJS **115**, 19 (1998), astro-ph/9704258.
[12] J. Harnois-Déraps, U.-L. Pen, I. T. Iliev, H. Merz, J. D. Emberson, and V. Desjacques, MNRAS **436**, 540 (2013), 1208.5098.
[13] A. Lewis, A. Challinor, and A. Lasenby, ApJ **538**, 473 (2000), astro-ph/9911177.
[14] H.-M. Zhu, Y. Yu, U.-L. Pen, X. Chen, and H.-R. Yu (in prep.).
[15] M. Tegmark, A. N. Taylor, and A. F. Heavens, ApJ **480**, 22 (1997), astro-ph/9603021.
[16] K. Akitsu, M. Takada, and Y. Li, ArXiv e-prints (2016), 1611.04723.
[17] R. Takahashi, N. Yoshida, M. Takada, T. Matsubara, N. Sugiyama, I. Kayo, A. J. Nishizawa, T. Nishimichi, S. Saito, and A. Taruya, ApJ **700**, 479 (2009), 0902.0371.
[18] M. C. Neyrinck, I. Szapudi, and C. D. Rimes, MNRAS **370**, L66 (2006), astro-ph/0604282.
[19] M. C. Neyrinck, in *Statistical Challenges in 21st Century Cosmology*, edited by A. Heavens, J.-L. Starck, and A. Krone-Martins (2014), vol. 306 of *IAU Symposium*, pp. 251–254, 1407.4815.
[20] D. J. Eisenstein, H.-J. Seo, E. Sirko, and D. N. Spergel, ApJ **664**, 675 (2007), astro-ph/0604362.
[21] M. White, MNRAS **450**, 3822 (2015), 1504.03677.